

Ocular neuroprotection by siRNA targeting caspase-2

Z Ahmed^{*,1,2,5}, H Kalinski^{3,5}, M Berry^{1,2}, M Almasieh⁴, H Ashush³, N Slager³, A Brafman³, I Spivak³, N Prasad¹, I Mett³, E Shalom³, E Alpert³, A Di Polo⁴, E Feinstein^{*,3,6} and A Logan^{1,2,6}

Retinal ganglion cell (RGC) loss after optic nerve damage is a hallmark of certain human ophthalmic diseases including ischemic optic neuropathy (ION) and glaucoma. In a rat model of optic nerve transection, in which 80% of RGCs are eliminated within 14 days, caspase-2 was found to be expressed and cleaved (activated) predominantly in RGC. Inhibition of caspase-2 expression by a chemically modified synthetic short interfering ribonucleic acid (siRNA) delivered by intravitreal administration significantly enhanced RGC survival over a period of at least 30 days. This exogenously delivered siRNA could be found in RGC and other types of retinal cells, persisted inside the retina for at least 1 month and mediated sequence-specific RNA interference without inducing an interferon response. Our results indicate that RGC apoptosis induced by optic nerve injury involves activation of caspase-2, and that synthetic siRNAs designed to inhibit expression of caspase-2 represent potential neuroprotective agents for intervention in human diseases involving RGC loss.

Cell Death and Disease (2011) 2, e173; doi:10.1038/cddis.2011.54; published online 16 June 2011

Subject Category: Neuroscience

Ocular neuroprotection, specifically the preservation of retinal ganglion cells (RGC), is of particular interest as numerous ocular pathologies, such as glaucoma and ischemic optic neuropathy (ION), cause permanent loss of RGC, leading to vision loss and blindness (for reviews see Schmidt *et al.*¹ and Kisiswa *et al.*²). RGCs are particularly susceptible possibly because retrograde axonal transport of target-derived neurotrophic factors to RGC somata via the optic nerve (ON) is compromised owing to damage to the ON in these pathologies.³ The ON transection model in adult rats initiates rapid onset and progression of RGC death and is considered suitable for studying mechanisms of RGC death and for testing the activity of neuroprotective compounds.^{4–7} In this model, apoptosis is thought to account for the death of the majority of RGC. Accordingly, treatments that inhibit apoptosis reduced the number of dying RGC in this model. These include microglial inhibitors,^{8,9} glial or brain-derived neurotrophic factors (BDNFs),¹⁰ implantation of activated macrophages,¹¹ over-expression of Bcl-2^{12,13} and caspase inhibitors such as the synthetic peptides Ac-Tyr-Val-Ala-Asp-aldehyde or benzyloxy-carbonyl-Asp-Glu-Val-Asp-chloromethylketone.^{14–16}

The caspases are a family of cysteine proteases that activate apoptotic pathways either as ‘initiators’ or ‘effectors’

(or ‘executioners’) based on their structural and functional characteristics. The initiator caspases cleave and activate executioner caspases (e.g. caspase-3 or -7), which, in turn, hydrolyse important proteins eventually inducing apoptosis. Caspase-2 is one of the most highly conserved caspases and is unique in that it can act as both an initiator and an effector caspase, depending on the apoptotic scenario.^{17–25} Structurally, caspase-2 is an initiator caspase because of its long pro-domain containing a caspase recruitment domain. Similar to other initiator caspases, activation of caspase-2 occurs via proximity-induced dimerization following recruitment to large protein complexes. After dimerization (aggregation), auto-cleavage of caspase-2 may take place, rendering it more active than the full-length dimerized enzyme. Although caspase-3-mediated cleavage of pro-caspase-2 has been described, it is not a caspase-2 activation event.^{26–29} In response to a variety of treatments, activation of caspase-2 occurs predominantly in the cytosol via recruitment to a protein complex termed PIDDosome acting downstream to mitochondria activation in apoptosis pathways.^{17–25} However, caspase-2 activation can also occur independent of PIDDosome and through death receptor pathways, such as those triggered by TRAIL or FAS.^{30–35} Unlike other initiator

¹Neuropharmacology and Neurobiology Section, School of Clinical and Experimental Medicine, College of Medical and Dental Sciences, University of Birmingham, Birmingham, UK; ²Neuregenix Ltd, The Research Park, Birmingham, UK; ³Quark Pharmaceuticals Inc. (Research Division), Weizmann Science Park, Ness Ziona, Israel and ⁴Department of Pathology and Cellular Biology, University of Montreal, Montreal, Quebec, Canada

*Corresponding authors: Z Ahmed, Neuropharmacology and Neurobiology Section, School of Clinical and Experimental Medicine, College of Medical and Dental Sciences, Room 2.17 2nd Floor, Institute of Biomedical Research (West), University of Birmingham, Edgbaston, Birmingham B15 2TT, UK. Tel: +44 121 414 8858; Fax: +44 121 414 8867; E-mail: z.ahmed.1@bham.ac.uk

or E Feinstein, Quark Pharmaceuticals Inc., Weizmann Science Park, POB 4071, Ness Ziona 70400, Israel. Tel: +972 8 8305113; Fax: +972 8 9406476; E-mail: efeinstein@quarkpharma.com

⁵These authors contributed equally to this work.

⁶Joint senior authors.

Keywords: synthetic siRNA; retinal ganglion cells; apoptosis; caspase-2; neuroprotection

Abbreviations: RGC, retinal ganglion cells; ION, ischemic optic neuropathy; siRNA, short interfering ribonucleic acid; RNA, ribonucleic acid; ON, optic nerve; BDNF, brain-derived neurotrophic factor; NAION, non-arteritic anterior ischemic optic neuropathy; ONC, optic nerve crush; INL, inner nuclear layer; siCASP2, short interfering RNA targeting caspase-2; FACS, fluorescence-activated cell sorting; RLM-RACE, RNA ligase-mediated rapid amplification of cDNA ends; PBS, phosphate-buffered saline; siCNL, short interfering RNA targeting control gene; FG, FluroGold; ONT, optic nerve transection; ANOVA, analysis of variance; siGFP, short interfering RNA targeting green fluorescent protein; VEGF, vascular endothelial growth factor; RNAi, RNA interference; LNA, locked nucleic acids

Received 08.10.10; revised 09.5.11; accepted 10.5.11; Edited by A Verkhratsky

caspases, caspase-2 does not directly activate the executioner caspases but, instead, signals death through activation of mitochondrial apoptosis; hence, functioning as its potential amplifier.^{36,37} The multifaceted participation of caspase-2 in apoptosis following a variety of stresses, including DNA damage, heat shock, stimulation of death receptors, cytoskeletal disruption, endoplasmic reticulum stress and oxidative stress,³⁸ makes it an attractive target for therapeutic intervention in diseases associated with pathological cell loss. For example, caspase-2-deficient neurons are resistant to apoptosis induced by β -amyloid^{39,40} and activation of caspase-2 is involved in apoptosis of hippocampal neurons following transient global ischemia in rats.⁴¹ Caspase-2 is expressed in RGC of ischemic retinas,⁴² and the neuroprotective effect of BDNF in this model is associated with reduced levels of caspase-2 immunohistochemical staining.⁴³ However, there is no previous literature indicating that caspase-2 is specifically involved in RGC death after ON injury.

These studies were aimed at evaluating the contribution of caspase-2 to RGC death in two adult rats ON injury models by characterizing its expression pattern post-injury, inhibiting its expression using caspase-2-specific short interfering ribonucleic acid (siRNA) and testing the potential of this siRNA as a novel neuroprotective agent. Here we show that after ON injury caspase-2 is cleaved in RGC, most likely as a result of pro-caspase-2 activation, and this cleavage represents an important feature of the resultant RGC death. We further show that inhibition of caspase-2 with an intravitreally administered synthetic chemically modified siRNA protects RGC from death after ON injury. The specific siRNA used in these rat studies is now being evaluated in clinical studies and is being developed for the treatment of ON injuries, including non-arteritic anterior ischemic optic neuropathy (NAION), an acute disease associated with RGC loss.

Results

Caspase-2 is expressed and cleaved in RGC after ON crush. We examined caspase-2 mRNA expression in retinas from either normal animals or animals subjected to ON crush (ONC), which leads to retrograde death of the entire RGC population by 21–30 days after the injury.^{44–49} Caspase-2 mRNA was found to be enriched in RGC compared with other types of cells in normal rat retinas as detected by quantitative RT-PCR (qPCR) analysis of Thy1.1-positive and -negative populations of retinal cells (Figure 1a and Supplementary Figure 1). To examine caspase-2 localization in RGC after ON damage, we performed comparative immunohistochemistry analysis in the ONC model. In retinas from normal animals, low levels of total caspase-2 protein were detected in a minority of RGC, and no caspase-2-specific signal was detected with the antibodies recognizing the cleaved version (upper panels of Figures 1d and f, respectively). In contrast, the cleaved form of caspase-2 was detectable in RGC one day after ONC, demonstrating that processing of caspase-2 is rapidly initiated in the retina after ON injury (Figures 1b and c). Detection of cleaved caspase-2 at this time point, albeit at abundance, correlated with the presence of few apoptotic

(TUNEL-positive) cells in the ganglion cell layer (GCL) (not shown). By day 7 after ONC, increased total (Figures 1d and e) and cleaved caspase-2 (Figures 1f and g) staining was observed in greater than 90% of RGC, suggesting that caspase-2 activation by both aggregation and subsequent cleavage has a role in RGC apoptosis in this model. Caspase-2 protein expression could also be detected in occasional cells of the inner nuclear layer (INL).

To distinguish whether enhanced total caspase-2 staining in RGC stemmed from the aggregation only or was also accompanied by increase in the protein levels, we performed western blot analysis and subsequent densitometry using protein extracts from retinas harvested at day 7 after ONC. The levels of both the pro- and cleaved forms of caspase-2 were elevated at 7 days after ONC compared with control intact retinas (Supplementary Figure 2). In particular, the 12 kDa cleaved fragment, which the antibody is directed against, was elevated by twofold over controls after ONC (Supplementary Figure 2b). These data demonstrated that both levels of pro-caspase-2 protein and accumulation of its cleaved form increased in rat retinas after ON injury.

As caspase-2 can be cleaved by caspase-3 without its subsequent activation,^{26–29} we performed immunohistochemical analysis on post-ONC retinal sections, adjacent to those shown in Figures 1d and f, and demonstrated that cleaved caspase-3 was neither localized to β III-tubulin-positive RGC (Supplementary Figure 3a) nor to GFAP-positive astrocytes (Supplementary Figure 3b) in the GCL, but rather was localized to cells in the INL (arrowheads), suggesting that caspase-3 was not responsible for RGC apoptosis nor the presence of cleaved caspase-2 in RGC and the latter was rather an indication of caspase-2 activation in these cells. Moreover, the time kinetics of the abundance of caspase-2 activation in RGC is in a good agreement with previously published data on the time kinetics of RGC apoptosis in the ONC model.^{4–7}

Properties of siRNA targeting caspase-2. To verify the functional involvement of caspase-2 in RGC apoptosis in the ONC model, and to explore the possible protective effects of caspase-2-targeted siRNAs in ON damage models of RGC death, we designed a chemically modified synthetic siRNA targeting caspase-2 (siCASP2) that is capable of inhibiting both the human and rat caspase-2 orthologues. siCASP2 was tested initially in cell culture by qPCR for its ability to elicit caspase-2 mRNA knockdown following transfection. In human HeLa cells, siCASP2 exhibited an IC_{50} against human caspase-2 mRNA of ~ 0.8 nM, and human caspase-2 mRNA levels could be reduced by over 80% (Figure 2a). Transfection of siCASP2 into rat PC12 cells reduced rat caspase-2 mRNA levels by 65% (Supplementary Figure 4a). This difference in potency of siCASP2 between human HeLa and rat PC12 cells may be explained by better accessibility of the siRNA target region in the human compared with the rat transcript due to local secondary structure (Supplementary Figure 5),⁵⁰ or may stem from other reasons such as potential differences in transfection efficiency or intrinsic RNA interference (RNAi) potency between HeLa and PC12 cells. The chemical modifications incorporated into siCASP2 conferred resistance to nucleases

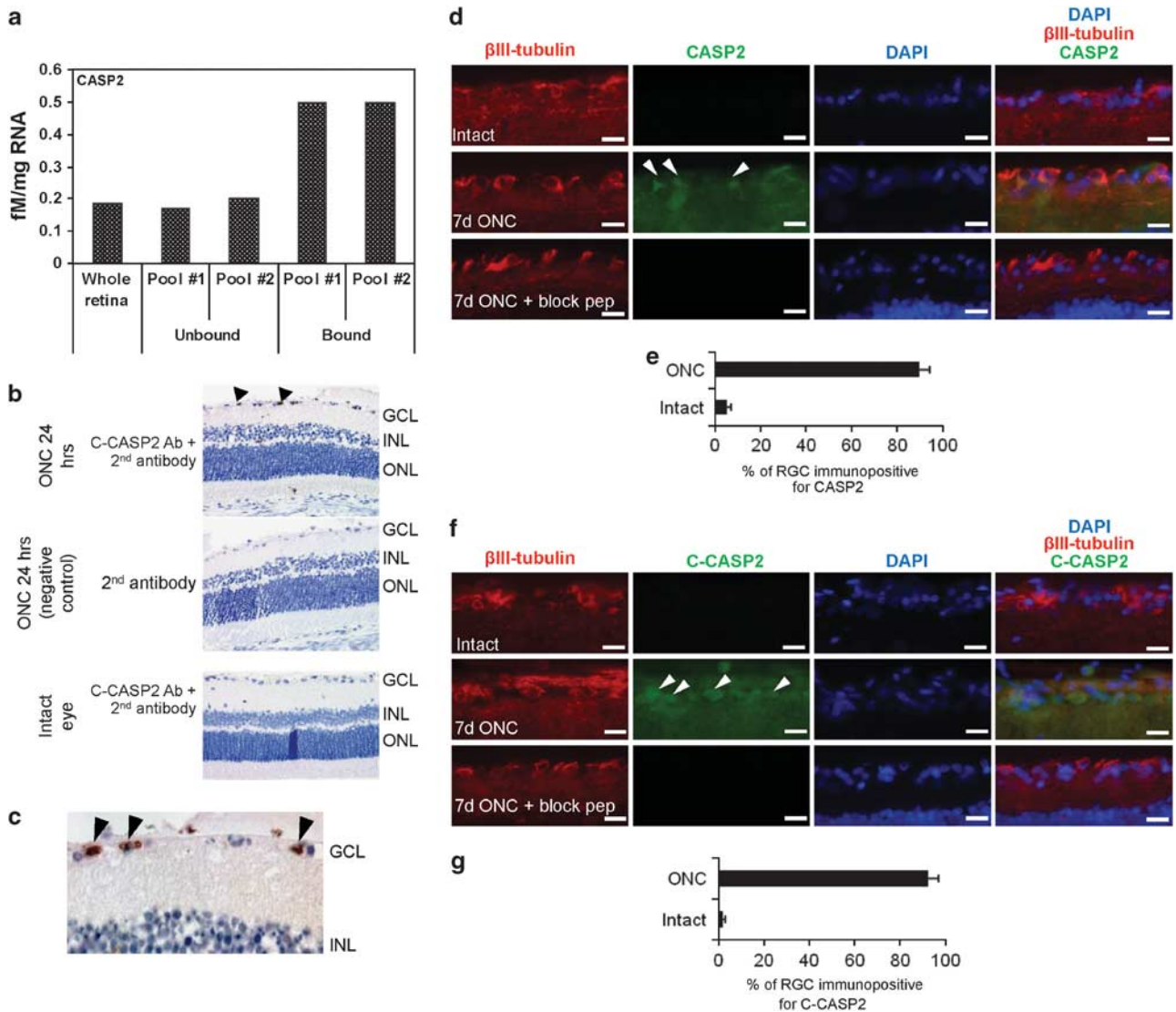


Figure 1 Caspase-2 is cleaved in RGC after ONC. (a) qPCR analysis of caspase-2 mRNA abundance in Thy1.1⁺ (bound to magnetic beads coupled to anti-Thy1.1 antibodies) and other retinal cells (unbound). (b) Representative microphotographs of sections of rat retina 24 h after ONC. Arrowheads show cleaved (p12) caspase-2 (C-CASP2) immunoreactivity (original magnification $\times 40$). (c) High-power images (original magnification $\times 63$) of top panel in (b) demonstrating cleaved caspase-2 (C-CASP2) immunoreactivity (brown) in the GCL (arrowheads). (d) Double immunohistochemical staining shows that CASP2 (green; arrowheads) is present in higher amounts at 7 days after ONC in RGC compared with intact control β III-tubulin-positive RGC (red). The blocking peptide used as a negative control gave no CASP2⁺ immunoreactivity. (e) Percentage of CASP2/ β III-tubulin-double-positive cells among β III-tubulin-positive cells, all in the ganglion cell layer \pm S.D. (i.e. RGC; calculations were made from 18 retinas per treatment and sampled from five different areas of each retina). (f) Double immunohistochemistry did not detect C-CASP2 (green) in RGC (red) of intact controls, but did localize C-CASP2 (colocalization = orange) in RGC at 7 days post-ONC scale bar (d) and (f) = 25 μ m; IHC = immunohistochemistry, GCL = ganglion cell layer, INL = inner nuclear layer, ONL = outer nuclear layer, IPL = inner plexiform layer, block pep = blocking peptide). (g) Percentage of β III-tubulin-positive cells in the ganglion cell layer (RGC) also containing C-CASP2 \pm S.D.

in serum (Supplementary Figure 4b) and vitreous humour (Figure 2b) for at least 24 h at 37 °C abrogating any potential seed- and passenger-strand-mediated off-target effects (Supplementary Figure 6), and blocked the ability of the siRNA to activate innate immune responses as confirmed by lack of *in vivo* interferon responses (Figure 2c) and *in vitro* cytokine production (Supplementary Figure 7).

siCASP2 is efficiently taken up by retinal cells *in vivo*. To determine the efficiency of uptake of siCASP2 in the retina following intravitreal administration, we injected

a fluorescent Cy3-labelled siRNA that contained chemical modifications similar to siCASP2 and monitored its distribution in the retina by fluorescence-activated cell sorting (FACS) analysis at 1 and 18 h after injection (Figure 3a). As evident, the whole Thy-1⁺ retinal cell population was positive for Cy3 staining, consistent with siRNA uptake (Figure 3a). Similar results were obtained by fluorescence microscopy. In retinal whole mounts, Cy3-labelled siRNA was found in up to 90% of retinal cells 5 h after intravitreal injection (Supplementary Figure 8a), and the fluorescent signal in these cells persisted for at least 24 h

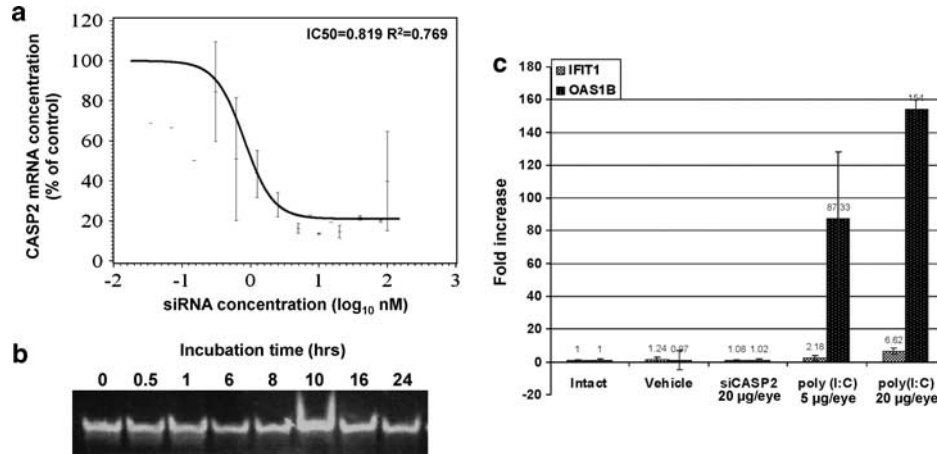


Figure 2 Target knockdown activity, nuclease stability and interferon response-inducing properties of siCASP2. (a) siCASP2 dose-dependent knockdown of caspase-2 mRNA in HeLa cells \pm S.D. (b) Analysis of siCASP2 integrity on native polyacrylamide gel following incubation *in silico* in rabbit vitreal fluid. '0' time point corresponds to siRNA aliquot dissolved in PBS (size control). (c) Induction of interferon (IFN)-responsive gene expression in rat retina/choroid after intravitreal injection of either 20 µg of siCASP2, 5–20 µg of poly(I:C) or PBS ($n = 3–10$), and the expression of IFN-responsive genes, IFIT1 and OAS1B 6 (not shown as no induction of gene expression was detected at this time point in any group) analysed 24 h later by quantitative RT-PCR. The results are expressed as % increase over control intact eyes (100%) (\pm S.D.) (IFIT1, interferon-induced protein with tetratricopeptide repeats 1; OAS1B 6, 2'-5'-oligoadenylate synthase 1B 6)

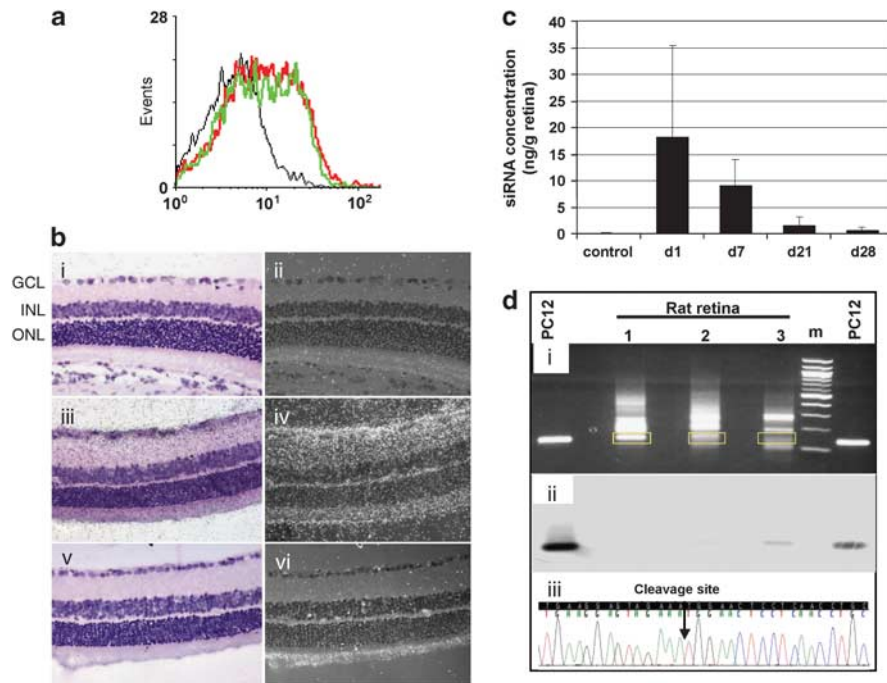


Figure 3 Localization, stability and RNAi activity of intravitreally injected siCASP2. (a) Detection of Cy3 fluorescence in isolated RGC 1 h (red line) or 18 h (green line) following single intravitreal injection of 40 µg Cy3-siRNA per rat eye. FACS analysis displaying results obtained from representative one out of two retinal tissue pools analysed per time point are shown. (b) Representative micro-autoradiographs of paraffin sections (counterstained with haematoxylin and eosin) from untreated ((i), (ii)) and siCASP2-injected rat eyes ((iii)–(iv)), which were hybridized with either siCASP2-specific ((i)–(iv)) or with a nonspecific ((v), (vi)) control ³³P-labelled probe ((i), (iii), (v)) – bright field images, ((ii), (iv), (vi)) – corresponding dark field images. In dark field images, hybridization signals are white dots over all retinal layers in sections of siCASP2-injected eyes hybridized to the specific probe ((iv)) and were especially prominent in the GCL (arrow). No signal in the GCL is detected in control sections ((ii), (vi)) (exposure 24 h, original magnification $\times 20$). The eyes for *in situ* hybridization analysis were enucleated at 2 h after intravitreal injection of 20 µg siRNA. At least 10 eyes from each group were analysed from 2 to 3 different experiments. (c) Quantification of siCASP2 \pm S.D. in retina at different times after intravitreal injection of 20 µg per eye siCASP2 ($n = 6$). Control retinas were obtained from intact non-injected eyes. (d) Detection of siCASP2-mediated RNAi using RLM-RACE: (i) EtBr-stained agarose gel with electrophoresed RLM-RACE products from siCASP2-transfected PC12 cells (size control) and from retinas collected at 4 h after intravitreal injection of PBS (1); 20 µg siCNL (2); or 20 µg siCASP2 (3) (yellow boxes indicate gel regions excised for cloning and subsequent colony sequencing); (ii) autoradiograph of the Southern blot of the gel shown in (i) after hybridization with radiolabelled RLM-RACE junction-specific probe; and (iii) example of the results of colony sequencing showing the RLM-RACE junction corresponding to the expected siCASP2 produced cleavage site. RLM-RACE was performed on RNA extracted from a pool of two retinas from eyes injected with PBS, pool of five retinas from the eyes injected with siCNL or a pool of four retinas from the eyes injected with siCASP2

(Supplementary Figure 8b). Similar distribution data to that obtained with Cy3-labelled siRNA were generated by *in situ* hybridization detection of siCASP2 in the retina using a radiolabelled siCASP2-specific oligonucleotide probe complementary to its guide strand. The highest intensity signal was observed in the GCL layer with lower intensity signal in other layers of the retina (Figure 3b). Intact siCASP2 was quantifiable in the retina by the 'Stem & Loop' qPCR method for as long as 28 days after a single intravitreal injection (Figure 3c). Thus, the intravitreal delivery route for targeting RGC is effective for siCASP2 as siCASP2 was found to be taken up rapidly by RGC and to persist in the retina for weeks. These data illustrate the remarkable stability of this chemically modified synthetic siRNA in eye tissues.

siCASP2 reduces caspase-2 mRNA in treated eyes. To demonstrate that siCASP2 reduces target mRNA expression in treated eyes is technically very demanding as RGC only constitute <1% of the total retinal cell population and caspase-2 mRNA expression level even in the enriched RGC population is extremely low (10-fold less than that of Thy1.1 mRNA and 100-fold less than NEFL mRNA – Figure 1a and Supplementary Figure 1b). Nonetheless, we dissected out retinæ from siCASP2- and control-treated eyes at either 72 or 96 h post-injection, immunopanned RGC using anti-Thy1.1 antibody-coupled beads (see Supplementary Material and Methods section for details) and performed qPCR analysis. We were able to demonstrate a ~50% reduction in caspase-2 mRNA level with siCASP2 treatment compared with control. However, these differences did not reach statistical significance (Supplementary Figures 9a and b).

siCASP2 induces specific RNAi-mediated caspase-2 mRNA cleavage *in vivo*. To verify that RNAi activity was induced by siCASP2 in rat retinas after intravitreal administration, we used the RNA ligase-mediated rapid amplification of cDNA ends (RLM-RACE) method to detect the presence of caspase-2 mRNA-specific cleavage product in rat retina. As evident from Figure 3d(ii), a band of the expected size was detected only in retina samples from rat eyes injected with siCASP2, and not from eyes injected with vehicle (PBS) or negative control short interfering RNA targeting control gene (siCNL). Cloning and sequencing of the RACE products generated using retinal mRNA from siCASP2-injected eyes and eluted from the gel (Figure 3c(i)) confirmed that cleavage occurred at the expected site in the caspase-2 mRNA (Figure 3d(iii)). In contrast, none of the 66 sequenced clones from vehicle-treated eyes and the 65 sequenced clones from control siCNL-treated eyes, obtained by the same procedure, contained the predicted siCASP2-mediated cleavage site.

siCASP2 protects RGC from apoptosis in two models of acute ON injury. The neuroprotective effect of siCASP2 was assessed by counting the number of FluoroGold (FG) back-labelled RGC in retinal whole mounts at 7 days^{51,52} after ONC or at 14 days after ON transection (axotomy) (ONT). In the ONC model, RGC axons were transected by

clamping, leaving the neural sheath and central retinal artery intact. In the ONT model, all RGC axons and neural sheath are completely severed without compromising the central retinal artery. ONT induces a more acute and rapid loss of RGC than ONC and is, therefore, a more aggressive model for evaluating RGC neuroprotection.⁵³

In eyes treated with the negative control siCNL, 60% RGC loss was apparent at 7 days post-ONC, whereas >90% of RGC were still intact in eyes injected with 5 µg of BDNF used as a positive control (Figures 4a and b). Single intravitreal administration of siCASP2 resulted in a dose-dependent increase in RGC survival between siRNA doses of 5 and 20 µg per eye. Doses of 20 and 35 µg per eye resulted in RGC densities that were comparable to that in intact retinas (~98% of RGC preserved). Doses above 35 µg per eye resulted in reduced RGC protection relative to the optimal doses of 20 and 35 µg per eye (Figures 4a and b). In spite of the reduced efficacy of high siCASP2 doses, a significant neuroprotective effect ($P < 0.01$, analysis of variance (ANOVA)) was apparent in all dose groups relative to the negative control. These results suggest that a single intravitreal administration of siCASP2 in the rat significantly protects RGC from apoptosis induced by ONC for at least 7 days. It is unclear as to why efficacy was reduced at doses above 35 µg as no overt toxicity was observed upon gross examination of the retinal whole mounts.

In eyes similarly treated with 20 µg of siCASP2 at days 0 and 10 after ONC, sustained neuroprotection was observed even on day 30: siCASP2 maintained the mean viability of 12-fold more RGC per mm² than in PBS-treated controls (Supplementary Figure 10). This equated to a mean survival of >8% of the total population of RGC found in control intact retinas compared with <1% survival in PBS-treated controls.

In the ONT model, 10 µg of siCASP2 or control siRNA targeting green fluorescent protein (siGFP) was administered twice by intravitreal injection – once immediately after ONT and again on day 7 post-ONT. Similar to the results obtained in the ONC model, neuroprotection was also observed with siCASP2 14 days after ONT in this more aggressive RGC injury model, where RGC densities were greater by up to 2.5-fold in eyes treated with siCASP2 relative to eyes treated with the negative control siRNA, siGFP ($P < 0.01$, ANOVA) (Figures 4c and d).

Discussion

Death of RGC is the main cause of blindness in several diseases, including glaucoma and NAION. ON injury models, such as those used in our studies, are a valuable tool for exploring mechanisms of RGC death and for screening potential neuroprotective agents.^{54–56} These models are technically convenient as RGC axons are easily accessible in the ON as a single population and therapeutic agents may be applied to the RGC somata through intraocular injections. The particular advantage of these models is that they allow quantitative assessment of the capacity of pharmacological agents to influence survival of RGCs after ON injury.^{57,58} Moreover, pharmacological agents showing neuroprotective efficacy in these very aggressive models can be expected to

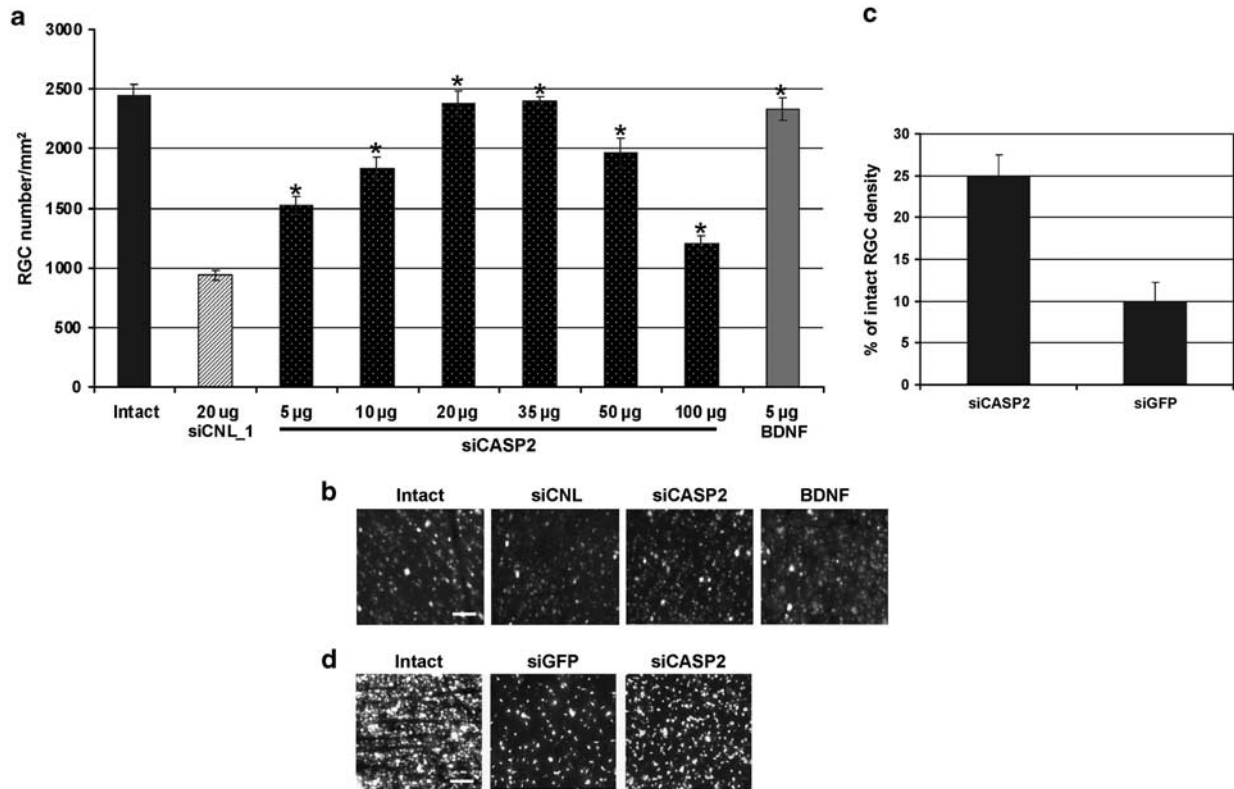


Figure 4 Protection of RGC from death by siCASP2 treatment after ONC and ONT. (a) Treatment with siCNL at 7 days post-ONC resulted in 60% RGC death compared with intact and BDNF-treated controls. Increasing the dose of siCASP2 from 5 to 20 µg enhanced RGC survival with 20–35 µg per eye, resulting in 100% RGC protection compared with intact and positive controls. (c) siCASP2 enhanced RGC survival by 15% after ONT compared with the protection afforded by a control siGFP at 14 days after ONT. (b) and (d) Representative FG back-labelled RGC in retinal whole mounts demonstrate the neuroprotection promoted by siCASP2 treatment after ONC and ONT, respectively (scale bars (b) and (d) = 100 µm). Note: the differences in FG labelling between (b) and (d) are due to the methodology used in the two different laboratories, please see Materials and Methods for full details

be efficient also in conditions of generally more mild ON injury typical for relevant human diseases.

The data reported here demonstrate that caspase-2 is activated and autocleaved specifically in RGC after ON injury. Both the pro- and the cleaved forms of the enzyme were found to be elevated in retinas of ONC eyes together with caspase-2 mRNA, indicating that the protein levels were also increased after injury.

A single intravitreal injection of a synthetic chemically modified siRNA targeting caspase-2 afforded almost complete protection of RGC during the first week after ONC, maintaining enhanced survival for 30 days after ONC, and significantly improved RGC survival in the more severe and prolonged ONT model. The magnitude of the neuroprotective effect of siCASP2 in the ONC model was comparable to that of BDNF. To date, BDNF administration has been the most effective neuroprotective strategy for preserving RGC for up to 7 days in the aggressive axotomy model.^{59,60} However, sustained RGC protection has not been observed with BDNF treatment⁶¹ owing to the rapid downregulation of its high-affinity receptor, TrkB, in response to the ON injury.^{62,63} Interestingly, published data suggest that the neuroprotective effects of BDNF after retinal ischemia may be partially mediated by BDNF-induced reduction of caspase-2 protein levels.⁶⁴

Synthetic siRNAs capable of inducing sequence-specific gene silencing are emerging as a potentially powerful new class of therapeutics. Synthetic siRNAs are comprised of short (15–27 bp) double-stranded RNA capable of guiding cleavage and subsequent degradation of target mRNAs via the RNAi pathway. The first clinical applications of RNAi-based therapies have been in wet age-related macular degeneration (wet AMD).⁶⁵ To date, only three synthetic siRNAs have been evaluated by direct intravitreal administration for their safety and efficacy in human beings – one non-modified siRNA ('Cand5' or 'bevasiranib'; Opko Pharmaceuticals, Miami, FL, USA) targeting vascular endothelial growth factor (VEGF), one partially modified siRNA ('Sirna027' or 'AGN211745'; Allergan (Irvine, CA, USA)/Sirna Therapeutics (San Francisco, CA, USA)/Merck (NJ, USA)) targeting its receptor VEGFR1 and a substantially modified siRNA ('RTP801' or 'PF-04523655'; Quark Pharmaceuticals/Pfizer, Ness Ziona, Israel) targeting RTP801/DDIT4. Clinical trials with the first two siRNAs have been discontinued owing to the lack of efficacy, whereas the siRNA targeting RTP801 is currently in Phase II clinical trials being conducted by Pfizer for the treatment of wet AMD and diabetic macular oedema.

Demonstration of the utility of RNAi in the eye using synthetic siRNAs has been complicated by the publication of Kleinman *et al.*,⁶⁶ where it was reported that 'naked'

(non-formulated) siRNAs are unable to enter retinal cells and exert RNAi without facilitating delivery by, for example, conjugation to cholesterol. Instead, the observed biological effects (i.e. antiangiogenic effects) were ascribed to triggering of toll-like receptor 3 that is a sensor for double-stranded RNA. Indeed, nonspecific effects associated with triggering innate immune and secondary interferon responses by non-modified siRNAs have been reported also in other systems.^{67–69} On the other hand, non-modified siRNAs are usually nuclease-labile and cannot persist in biological fluids for prolonged times, which too might contribute to their reduced *in vivo* uptake and activity. However, chemical modifications can be used to both stabilize synthetic siRNA against nuclease degradation and to abrogate its off-target and immunostimulatory effects. Synthetic siRNAs containing 2'-*O*-methyl, 2'-fluoro, 2'-deoxy or locked nucleic acid (LNA) nucleotides have been shown to be protected from rapid nuclease degradation, thus enhancing the longevity of the gene silencing function (reviewed in Robbins *et al.*⁷⁰). Furthermore, selective incorporation of 2'-*O*-methyl guanosine or 2'-*O*-methyl uridine residues in the passenger strands of highly immunostimulatory siRNA molecules completely abrogated siRNA-mediated interferon responses.⁷¹

The synthetic chemically stabilized siRNA targeting caspase-2 reported here was shown to: (1) be resistant to nuclease degradation, allowing it to persist in rat retina for up to 28 days after intravitreal administration; (2) be taken up effectively by the cells in the rat retina following intravitreal administration, with the highest accumulation in RGC; (3) not elicit any interferon or cytokine responses; (4) not exhibit seed-mediated or passenger-strand mediated off-target effects; and (5) elicit RNAi-mediated cleavage of caspase-2 mRNA *in vivo*. These properties support the clinical development of siCASP2 described in this communication for ocular neuroprotection. This siCASP2 is currently being evaluated in the clinic as a neuroprotective agent for the treatment of sudden vision loss associated with NAION, and non-invasive delivery strategies are being developed for the potential use of this siRNA to treat glaucoma.

To the best of our knowledge, the studies reported here are the first to explore the potential neuroprotective effects of intravitreally injected synthetic siRNAs. Only one previous report has described the use of non-modified siRNA for the purpose of ocular neuroprotection.⁷² However, the authors injected siRNAs directly into the ON stump for retrograde delivery to RGC, an administration route that is not readily clinically tractable. In contrast, we demonstrate for the first time that synthetic chemically stabilized siRNA can be delivered to RGC using a clinically relevant delivery route (intravitreal injection) to exert a strong neuroprotective effect. The fact that the 'naked' (unformulated) siRNA is taken up efficiently after intraocular delivery has an added advantage, eliminating the need for liposomal and/or viral delivery of the therapeutic siRNA/short hairpin RNA, thus avoiding potential safety issues associated with these strategies.⁷³

In conclusion, our results implicate caspase-2 as the predominant caspase responsible for the death of RGC after ON injury. Our results also show that stabilized siCASP2 exhibits a long residence time in the rat eye after intravitreal administration, is taken up readily by RGC, activates RNAi, is

neuroprotective after RGC axotomy and, therefore, may be a useful therapeutic in ophthalmic diseases that involve RGC death.

Materials and Methods

Animal care and procedures. Depending on the site of performance, animal procedures were evaluated and licensed by the UK Home Office and approved by the University of Birmingham Institutional Ethical Review Committee (AL Laboratory), or were reviewed and approved by Canadian Council on Animal Care (ADP Laboratory) for the use of experimental animals, or were reviewed and approved by the Hebrew University Animal Research Committee in Israel (Quark Laboratories).

siRNA. All siRNA molecules used in this study were similarly chemically stabilized and were synthesized at BioSpring (Frankfurt, Germany). siCASP2 had sequence 5'-GCCAGAAUGUGGAACUCCU-3' (sense strand) and was used in all relevant experiments described in this manuscript. Tracer siRNA having sequence 5'-GUGCCAACCUUGAUGCAGCU-3' (sense strand) and Cy3 fluorophore at the 3' end of the antisense strand was utilized for fluorescent microscopy. Control siRNA against GFP had sequence as described previously.⁷⁴ Another control siRNA, siCNL (sense strand: 5'-ACUAAUUACGCGCAUGC-3'), was generated by random combination of nucleotides and verified (using Smith–Waterman sequence comparison algorithm) for the lack of any similarity to human, rat and mouse transcriptome (RefSeq, NCBI).

siCASP2 stability in vitreous fluid. To monitor siCASP2 degradation by nucleases in the vitreous, siCASP2 was diluted in Dutch-belted rabbit vitreous (Bioreclamation, Hicksville, NY, USA) to a final concentration of 7 μ M (86 μ g/ml) and incubated at 37 °C. At time points between 0 and 24 h after incubation, 5 μ l aliquots were transferred to 15 μ l of 1.5 \times TBE-loading buffer, snap frozen in liquid N₂ and stored at –80 °C until use. The aliquots were thawed on ice and analysed on 20% non-denaturing polyacrylamide gel in a TBE buffer. Samples were visualized on an UV-transilluminator subsequent to ethidium bromide staining.

ONC model and counting of RGC. Adult, female 200–250 g Wistar rats ($n=4$ eyes per treatment) were anaesthetized intraperitoneally with Hypnorm/Hypnovel anaesthetic (Janssen Pharmaceuticals, Oxford, UK) and the ON of both eyes were crushed (ONC) intraorbitally to completely transect all RGC axons leaving sheath and artery intact. All reagents were intravitreally injected using glass micropipettes in a final volume of 10 μ l. Animals were treated with either PBS or with 20 μ g control siCNL or with 5, 10 or 20 μ g siCASP2 or with 5 μ g BDNF (Peprotech Ltd, London, UK) immediately after ONC and within 5 min post-surgery.

At 5 days post-ONC, 2 μ l of 4% FG (Cambridge Bioscience, Cambridge, UK) retrograde tracer was injected into the nerve mid-way between the lamina cribrosa and the site of ONC. After 48 h, animals were killed by exposure to CO₂ and intracardially perfused with 4% formaldehyde (TAAB Laboratories, Aldermaston, UK). Retinas were dissected out and immersion fixed in 4% formaldehyde (TAAB Laboratories) for 30 min and whole-mounted onto glass slides (VWR International, Lutterworth, UK). Four equidistal radial cuts were made to give four equally sized quadrants, attached together around the optic disc. Retinal whole mounts were air dried and mounted in Vectashield mounting medium (Vector Laboratories, Peterborough, UK). An observer was blinded to the treatments and groups and samples were randomly assigned numbers before image capture and analysis. Images were captured at $\times 20$ magnification using a Zeiss epifluorescent microscope (Zeiss, Hertfordshire, UK) equipped with a Axiocam HRc camera (Zeiss) running the Axiovision software (Zeiss). Images were captured from three different areas of each quadrant (total = 12 counts per quadrant, $n=4$ retinas per treatment, to account for variation of RGC numbers in the different areas and quantified using the built-in particle counting facilities in ImagePro; Media Cybernetics, Bethesda, MD, USA) and expressed as the number of RGC per mm² \pm S.E.M.

ONT model and counting of RGCs. RGCs were labelled by application of FG in the superior colliculus of adult female Sprague–Dawley rats (180–200 g) ($n=5–6$ per group). Both superior colliculi were exposed and a small piece of gel foam soaked in FG was applied to their surface as described previously.^{75–77} After 1 week, the entire population of RGCs in the left eye was axotomized by transecting the ON 0.5–1 mm posterior to the globe. With the aid of a standard, upright

operating microscope, the retinal vasculature was examined to confirm the integrity of the retinal circulation after each axotomy. Animals showing signs of compromised blood supply, identified by the collapse of vessels in the retinal vasculature and/or absence of blood flow, were excluded from the study. Intravitreal injections of 10 $\mu\text{g}/5 \mu\text{l}$ siCASP2 or 10 $\mu\text{g}/5 \mu\text{l}$ siGFP (both in PBS vehicle) were performed immediately following the axotomy procedure and then (for the 2nd time) at 7 days post-axotomy into the vitreous body of the left eye. Surgical glue (Indermill, Tyco Health Care, Mansfield, MA, USA) was used to seal the site of injection. Experimental and control animals (including those that did not undergo axotomy) were perfused transcardially with 4% paraformaldehyde 2 weeks after axotomy. Both eyes were dissected out and post-fixed in 4% paraformaldehyde for an additional 30 min at 4 °C. Fixed retinas were flat-mounted on Fisherbrand microscope slides. An observer was blinded to the treatment groups and samples were randomly assigned numbers before image capture and analysis. Fluorescence was visualized with a Zeiss Axioskop 2 Plus microscope (Carl Zeiss, Kirkland, QC, Canada), images were captured with a CCD camera (Retiga (Qimaging), Surrey, BC, Canada) and processed with the Northern Eclipse image analysis software (Empix Imaging, Mississauga, ON, Canada). Microphotographs were taken at $\times 25$ magnification. RGCs were counted in standard retinal areas as described previously^{75–77} and expressed as the number of RGC per $\text{mm}^2 \pm \text{S.E.M.}$

In situ hybridization detection of siRNA. The method used was based on the procedure described by Nelson *et al.*⁷⁸ with some modifications. The hybridization probes were single-stranded oligonucleotides in which every third position had LNAs. Their primary sequence corresponded to the sense strand of siCASP2 or siCNL siRNAs. The oligonucleotide probes were end labelled with [γ -³³P]ATP (Easytides ATP; Perkin-Elmer, Waltham, MA, USA) using polynucleotide kinase (New England Biolabs, Ipswich, MA, USA). In all, 10- μm -thick sections of eyes were deparaffinized, re-hydrated in decreasing concentrations of ethanol, de-proteinized with proteinase K, post-fixed in 10% NBF, acetylated in triethanolamine-acetic anhydride solution, washed in double-distilled water and air-dried. The eye sections were hybridized overnight at 48 °C in hybridization buffer containing 50% formamide, 10% dextran sulphate, $4 \times \text{SSC}$, $1 \times \text{Denhardt's}$ solution, 0.25 mg/ml salmon sperm DNA, 0.25 mg/ml tRNA and 20 nM of single-stranded LNA-modified siCASP2 or siCNL hybridization probes. Representative sections from intact and injected eyes were present on the same slide during the hybridization process. Following hybridization, the slides were sequentially washed in $5 \times \text{SSC}$, $2 \times \text{SSC}$, double-distilled water and air-dried. The hybridized slides were immersed in photographic emulsion for the periods between 4 h and up to 1 week, developed and analysed using a Zeiss Axioskop 2 light microscope (Carl Zeiss, Thornwood, NY, USA). The images were taken by Spot RT colour camera (Diagnostic Instruments Inc., Sterling Heights, MI, USA).

Cy3-siRNA detection in isolated RGC. A measure of 40 μg of Cy3-labelled tracer siRNA in 10 μl PBS vehicle was injected bilaterally into the vitreous body of four rats. After 1 or 18 h, rats were killed and the injected eyes were enucleated from two rats per time point and both dissected retinas from the same animal were transferred to a tube filled with PBS containing Ca^{2+} and Mg^{2+} . Cells from each of the two retinal pools were dissociated using 'Neural Tissue-Dissociation Kit – Postnatal Neurons' (Miltenyi Biotec, Auburn, CA, USA; cat. no. 130-094-802) as described in the manufacturer's protocol. Macrophages were depleted from the retinal cell suspension by attachment to Anti-Mouse CD11b Magnetic Particles (BD Biosciences, Franklin Lakes, NJ, USA; cat. no. 558013). RGCs were next separated using Thy-1 (CD90.1) Microbeads (Miltenyi; cat. no. 130-094-523). Cells were then stained with anti-rat Thy-1 (CD90.1) PerCP-Cy5.5 antibody, and Cy3-siRNA was observed in Thy-1-positive cell population (gated in Figure 3a) using FACS FL-2 and FL-3 filters.

Quantitation of siCASP2 in retinas. siCASP2 (35 μg per eye) was delivered by intravitreal injection to the left eyes of adult male Sprague–Dawley rats ($n = 4–6$). Rats were euthanized on days 1, 7, 21 or 28 days after the siRNA injections. Eyes were enucleated and the retinas were carefully separated from the sclera. Retinas were similarly collected from six untreated rats. Whole retinas were washed in a large volume of ice-cold PBS and RNA was extracted using EZ-RNA RNA extraction kit (Biological Industries, Kibbutz Beit-Haemek, Israel). The quantity of siCASP2 in each of the RNA samples was determined using the Stem & Loop qPCR method.⁷⁹ cDNA was synthesized using 1 μg RNA from each sample as template, a Stem & Loop structured primer (5'-GTCGTATCCAGTCCAGGGTCCGAGGTATTCGACTGGATACGACGCCAGA-3') and Superscript II Reverse

Transcriptase enzyme (Invitrogen, Carlsbad, CA, USA). qPCR was then carried out using SYBR Green Master Mix (ABI, New York, NY, USA) and two amplification primers: 5'-GGCGGAGGAGTCCACATTC-3' (forward) and 5'-GTGCAGGGTCCGAGGT-3' (reverse). siRNA quantity was determined by interpolation to a standard curve generated by qPCR amplification of a dilution series of siCASP2 spiked into normal retina RNA. Measured siRNA quantities were normalized to the geometric mean of mRNA levels of two reference genes, *rat cyclophilin A* (Genway, San Diego, CA, USA) and *rat β -actin*, which were determined in each sample by qPCR. Determined siRNA concentration was recalculated per gram retina.

In vivo detection of siCASP2-specific caspase-2 mRNA cleavage by RLM-RACE. Adult male 180–220 g Sprague–Dawley rats ($N = 4$ per treatment group) were subjected to intravitreal injection with 20 μg of siCASP2 or siCNL (non-targeting negative control) in 10 μl PBS per eye or with 10 μl PBS alone. After 4 h, retinas were harvested and extracted RNA was subjected to RLM-RACE analysis for the detection of siCASP2-produced mRNA cleavage product using Invitrogen GeneRacer Kit, according to the manufacturer's instructions. The following primers were used for amplification of the caspase-2-RACE-product, 5'-TCTGTGGATAGCGGGACTGCT-3'; 5'-GTGAGCAGTAAGTCTTCCAAGTG-3' (caspase-2-specific reverse PCR primer); 5'-GAGAGGGTTGTGAGCAGTAAGT-3' (caspase-2-specific nested reverse PCR primer); 5'-CGACTGGAGC ACGAGGACACTGCAT-3' (adapter-specific forward PCR primer); and 5'-G GACTGCATGGACTGAAGGAGTA-3' (adapter-specific nested forward PCR primer). RNA samples extracted from cultured PC12 cells transfected with siCASP2 were used as a positive control. RACE products were separated on preparative and analytical 2% agarose gels. The preparative gel was stained with ethidium bromide for RACE product visualization. The regions of the gel corresponding to the predicted size of the RACE amplification product were excised and DNA was extracted using QIAEX II agarose gel extraction kit (Qiagen, Valencia, CA, USA). In all, 5 ng of each DNA extract were used for cloning into pGEM-T Vector (Promega, Madison, WI, USA). Bacterial colonies harbouring insert-containing plasmids were isolated and their inserts sequenced to confirm the presence of the expected adaptor-caspase-2 mRNA junction. The analytical gel was blotted onto a Hybond N membrane and the blot was hybridized with a RACE product-specific oligonucleotide probe (5'-GGAGTAGAAATGGAAGTCT-3') labelled with [γ -³³P]ATP (Perkin-Elmer). The hybridization reaction was conducted overnight at 42 °C in a hybridization buffer ($6 \times \text{SSC}$, $1 \times \text{Denhardt's}$ solution (Invitrogen), 0.5% SDS, 0.05% NaPPi ($\text{Na}_4\text{P}_2\text{O}_7$) (Sigma, St. Louis, MO, USA) and 200 $\mu\text{g}/\text{ml}$ sonicated salmon sperm DNA (Sigma)). Following hybridization, the membrane was washed $3 \times$ for 15 min each at room temperature in $2 \times \text{SSC}$, 0.5% SDS solution and then exposed overnight to a KODAK BioMax film (Kodak, Rochester, NY, USA).

Conflict of Interest

Some of the authors (HK, HA, NS, AB, IS, IM, ES, EA and EF) are employees of a biopharmaceutical company (Quark Pharmaceuticals Inc.). The academic collaborators (AL and ADP laboratories) received funding from Quark and these funds were used towards project consumables, support staff salaries and attendance at symposia meetings. The study was designed and analysed with participation of the funding body. Nevertheless, none of this influenced the objectivity and integrity of the experiments and this publication.

Acknowledgements. This work was funded by Quark Pharmaceuticals Inc. and the Wellcome Trust Grant Nos. 065920 (to AL and MB) and 092539 (to ZA). We thank Drs Andy Thewles and Michael Douglas and Mr Imran Masood (all from University of Birmingham) for their technical assistance in animal surgery and immunohistochemistry, as well as members of the Cell Biology, Molecular Biology, Quantitative Real-Time PCR, Histopathology and Statistics groups from Quark Pharmaceuticals Inc. for excellent technical support, Drs Rami Skaliter and James Thomson from Quark Pharmaceuticals for helpful discussions and Dr James Thompson for critical reading and editing of the manuscript.

- Schmidt KG, Bergert H, Funk RH. Neurodegenerative diseases of the retina and potential for protection and recovery. *Curr Neuropharmacol* 2008; 6: 164–178.
- Kiswisa L, Dervan AG, Albon J, Morgan JE, Wride MA. Retinal ganglion cell death postponed: giving apoptosis a break? *Ophthalmic Res* 2010; 43: 61–78.

3. Johnson EC, Guo Y, Cepurna WO, Morrison JC. Neurotrophin roles in retinal ganglion cell survival: lessons from rat glaucoma models. *Exp Eye Res* 2009; **88**: 808–815.
4. Berkelaar M, Clarke DB, Wang YC, Bray GM, Aguayo AJ. Axotomy results in delayed death and apoptosis of retinal ganglion-cells in adult-rats. *J Neurosci* 1994; **14**: 4368–4374.
5. PeinadoRamon P, Salvador M, Villegasperez MP, Vidalsanz M. Effects of axotomy and intraocular administration of NT-4, NT-3, and brain-derived neurotrophic factor on the survival of adult rat retinal ganglion cells – a quantitative *in vivo* study. *Invest Ophthalmol Vis Sci* 1996; **37**: 489–500.
6. Villegasperez MP, Vidalsanz M, Rasminsky M, Bray GM, Aguayo AJ. Rapid and protracted phases of retinal ganglion-cell loss follow axotomy in the optic-nerve of adult-rats. *J Neurobiol* 1993; **24**: 23–36.
7. Isenmann S, Klockner N, Gravel C, Bahr M. Protection of axotomized retinal ganglion cells by adenovirally delivered BDNF *in vivo*. *Eur J Neurosci* 1998; **10**: 2751–2756.
8. Thanos S, Mey J, Wild M. Treatment of the adult retina with microglia-suppressing factors retards axotomy-induced neuronal degradation and enhances axonal regeneration *in vivo* and *in vitro*. *J Neurosci* 1993; **13**: 455–466.
9. Mey J, Thanos S. Intravitreal injections of neurotrophic factors support the survival of axotomized retinal ganglion-cells in adult-rats *in vivo*. *Brain Res* 1993; **602**: 304–317.
10. Koerber PD, Ball AK. Effects of GDNF on retinal ganglion cell survival following axotomy. *Vision Res* 1998; **38**: 1505–1515.
11. LazarovSpiegler O, Solomon AS, ZeevBrann AB, Hirschberg DL, Lavie V, Schwartz M. Transplantation of activated macrophages overcomes central nervous system regrowth failure. *FASEB J* 1996; **10**: 1296–1302.
12. Bonfanti L, Strettoi E, Chierzi S, Cenni MC, Liu XH, Martinou JC *et al*. Protection of retinal ganglion cells from natural and axotomy-induced cell death in neonatal transgenic mice overexpressing bcl-2. *J Neurosci* 1996; **16**: 4186–4194.
13. Chierzi S, Cenni MC, Maffei L, Pizzorusso T, Porciatti V, Ratto GM *et al*. Protection of retinal ganglion cells and preservation of function after optic nerve lesion in bcl-2 transgenic mice. *Vision Res* 1998; **38**: 1537–1543.
14. Kermer P, Klockner N, Labes M, Bahr M. CPP32-like proteases are major mediators of apoptosis in axotomized retinal ganglion cells *in vivo*. *Eur J Neurosci* 1998; **10**: 202.
15. Kermer P, Klockner N, Labes M, Bahr M. Inhibition of CPP32-like proteases rescues axotomized retinal ganglion cells from secondary cell death *in vivo*. *J Neurosci* 1998; **18**: 4656–4662.
16. Lucius R, Sievers J. YVAD protect post-natal retinal ganglion cells against axotomy-induced but not free radical-induced axonal degeneration *in vitro*. *Mol Brain Res* 1997; **48**: 181–184.
17. Lamkanfi M, Declercq W, Kalai M, Saelens X, Vandenabeele P. Alice in caspase land. A phylogenetic analysis of caspases from worm to man. *Cell Death Differ* 2002; **9**: 358–361.
18. Lassus P, Opitz-Araya X, Lazebnik Y. Requirement for caspase-2 in stress-induced apoptosis before mitochondrial permeabilization. *Science* 2002; **297**: 1352–1354.
19. Robertson JD, Enoksson M, Suomela M, Zhivotovskiy B, Orrenius S. Caspase-2 acts upstream of mitochondria to promote cytochrome c release during etoposide-induced apoptosis. *J Biol Chem* 2002; **277**: 29803–29809.
20. Kumar S, Vaux DL. Apoptosis. A Cinderella caspase takes center stage. *Science* 2002; **297**: 1290–1291.
21. Ho LH, Read SH, Dorstyn L, Lambrusco L, Kumar S. Caspase-2 is required for cell death induced by cytoskeletal disruption. *Oncogene* 2008; **27**: 3393–3404.
22. Tu S, McStay GP, Boucher LM, Mak T, Beere HM, Green DR. In situ trapping of activated initiator caspases reveals a role for caspase-2 in heat shock-induced apoptosis. *Nat Cell Biol* 2006; **8**: 72–77.
23. Tinel A, Tschopp J. The PIDDosome, a protein complex implicated in activation of caspase-2 in response to genotoxic stress. *Science* 2004; **304**: 843–846.
24. Sidi S, Sanda T, Kennedy RD, Hagen AT, Jette CA, Hoffmans R *et al*. Chk1 suppresses a caspase-2 apoptotic response to DNA damage that bypasses p53, Bcl-2, and caspase-3. *Cell* 2008; **133**: 864–877.
25. Upton JP, Austgen K, Nishino M, Coakley KM, Hagen A, Han D *et al*. Caspase-2 cleavage of BID is a critical apoptotic signal downstream of endoplasmic reticulum stress. *Mol Cell Biol* 2008; **28**: 3943–3951.
26. Harvey NL, Trapani JA, Fernandes-Alnemri T, Litwack G, Alnemri ES, Kumar S. Processing of the Nedd2 precursor by ICE-like proteases and granzyme B. *Genes Cells* 1996; **1**: 673–685.
27. Manzi C, Krumschnabel G, Bock F, Sohm B, Labi V, Baumgartner F. Caspase-2 activation in the absence of PIDDosome formation. *J Cell Biol* 2009; **185**: 291–303.
28. Kumar S. Caspase 2 in apoptosis, the DNA damage response and tumour suppression: enigma no more? *Nat Rev Cancer* 2009; **9**: 897–903.
29. Krumschnabel G, Sohm B, Bock F, Manzi C, Villunger A. The enigma of caspase-2: the laymen's view. *Cell Death Differ* 2009; **16**: 195–207.
30. Wagner KW, Engels IH, Deveraux QL. Caspase-2 can function upstream of bid cleavage in the TRAIL apoptosis pathway. *J Biol Chem* 2004; **279**: 35047–35052.
31. Droin N, Bichat F, Rebe C, Wotawa A, Sordet O, Hammann A. Involvement of caspase-2 long isoform in Fas-mediated cell death of human leukemic cells. *Blood* 2001; **97**: 1835–1844.
32. Duan H, Dixit VM. RAIDD is a new 'death' adaptor molecule. *Nature* 1997; **385**: 86–89.
33. Lavrik IN, Golks A, Baumann S, Kramer PH. Caspase-2 is activated at the CD95 death-inducing signaling complex in the course of CD95-induced apoptosis. *Blood* 2006; **108**: 559–565.
34. Olsson M, Vakifahmetoglu H, Abruzzo PM, Hogstrand K, Grandien A, Zhivotovskiy B. DISC-mediated activation of caspase-2 in DNA damage-induced apoptosis. *Oncogene* 2009; **28**: 1949–1959.
35. Manzi C, Krumschnabel G, Bock F, Sohm B, Labi V, Baumgartner F. Caspase-2 activation in the absence of PIDDosome formation. *J Cell Biol* 2009; **185**: 291–303.
36. Baliga BC, Read SH, Kumar S. The biochemical mechanism of caspase-2 activation. *Cell Death Differ* 2004; **11**: 1234–1241.
37. Bouchier-Hayes L, Oberst A, McStay GP, Connell S, Tait SW, Dillon CP *et al*. Characterization of cytoplasmic caspase-2 activation by induced proximity. *Mol Cell* 2009; **35**: 830–840.
38. Ho LH, Read SH, Dorstyn L, Lambrusco L, Kumar S. Caspase-2 is required for cell death induced by cytoskeletal disruption. *Oncogene* 2008; **27**: 3393–3404.
39. Troy CM, Rabacchi SA, Friedman WJ, Frappier TF, Brown K, Shelanski ML. Caspase-2 mediates neuronal cell death induced by beta-amyloid. *J Neurosci* 2000; **20**: 1386–1392.
40. Troy CM, Ribe EM. Caspase-2: vestigial remnant or master regulator? *Sci Signal* 2008; **1**: e42.
41. Niizuma K, Endo H, Nito C, Myer DJ, Kim GS, Chan PH. The PIDDosome mediates delayed death of hippocampal CA1 neurons after transient global cerebral ischemia in rats. *Proc Natl Acad Sci USA* 2008; **105**: 16368–16373.
42. Singh M, Savitz SI, Hoque R, Gupta G, Roth S, Rosenbaum PS *et al*. Cell-specific caspase expression by different neuronal phenotypes in transient retinal ischemia. *J Neurochem* 2001; **77**: 466–475.
43. Kurokawa T, Katai N, Shibuki H, Kuroiwa S, Kurimoto Y, Nakayama C *et al*. BDNF diminishes caspase-2 but not c-Jun immunoreactivity of neurons in retinal ganglion cell layer after transient ischemia. *Invest Ophthalmol Vis Sci* 1999; **40**: 3006–3011.
44. Berry M, Carille J, Hunter A. Peripheral nerve explants grafted into the vitreous body of the eye promote the regeneration of retinal ganglion cell axons severed in the optic nerve. *J Neurocytol* 1996; **25**: 147–170.
45. Berry M, Carille J, Hunter A, Tsang W, Rosustrel P, Sievers J. Optic nerve regeneration after intravitreal peripheral nerve implants: trajectories of axons regrowing through the optic chiasm into the optic tracts. *J Neurocytol* 1999; **28**: 721–741.
46. Ahmed Z, Suggate EL, Brown ER, Dent RG, Armstrong SJ, Barrett LB *et al*. Schwann cell-derived factor-induced modulation of the NgR/p75(NTR)/EGFR axis disinhibits axon growth through CNS myelin *in vivo* and *in vitro*. *Brain* 2006; **129**: 1517–1533.
47. Ahmed Z, Dent RG, Leadbeater WE, Smith C, Berry M, Logan A. Matrix metalloproteases: degradation of the inhibitory environment of the transected optic nerve and the scar by regenerating axons. *Mol Cell Neurosci* 2005; **28**: 64–78.
48. Douglas MR, Morrison KC, Jacques SJ, Leadbeater WE, Gonzalez AM, Berry M *et al*. Off-target effects of epidermal growth factor receptor antagonists mediate retinal ganglion cell disinhibited axon growth. *Brain* 2009; **132**: 3102–3121.
49. Logan A, Ahmed Z, Baird A, Gonzalez AM, Berry M. Neurotrophic factor synergy is required for neuronal survival and disinhibited axon regeneration after CNS injury. *Brain* 2006; **129**: 490–502.
50. Schubert S, Grunweller A, Erdmann VA, Kurreck J. Local RNA target structure influences siRNA efficacy: systematic analysis of intentionally designed binding regions. *J Mol Biol* 2005; **348**: 883–893.
51. Berry M, Carille J, Hunter A. Peripheral nerve explants grafted into the vitreous body of the eye promote the regeneration of retinal ganglion cell axons severed in the optic nerve. *J Neurocytol* 1996; **25**: 147–170.
52. Berry M, Carille J, Hunter A, Tsang W, Rosustrel P, Sievers J. Optic nerve regeneration after intravitreal peripheral nerve implants: trajectories of axons regrowing through the optic chiasm into the optic tracts. *J Neurocytol* 1999; **28**: 721–741.
53. Agudo M, Perez-Marín MC, Lonngren U, Sobrado P, Conesa A, Canovas I *et al*. Time course profiling of the retinal transcriptome after optic nerve transection and optic nerve crush. *Mol Vision* 2008; **14**: 1050–1063.
54. Kerr NM, Chew SS, Danesh-Meyer HV. Non-arteritic anterior ischaemic optic neuropathy: a review and update. *J Clin Neurosci* 2009; **16**: 994–1000.
55. Philips B, Dralands L, Missotten L. Non-arteritic anterior ischemic optic neuropathy and refraction. *Bull Soc Belge Ophthalmol* 1995; **259**: 183–187.
56. Verit A. Non-arteritic anterior ischemic optic neuropathy, PDE-5 inhibitors, and amiodarone: may there be a sex hormone effect for the eye? *Med Hypotheses* 2007; **69**: 470–471.
57. Zhang D, Sucher NJ, Lipton SA. Co-expression of AMPA/kainate receptor-operated channels with high and low Ca²⁺ permeability in single rat retinal ganglion cells. *Neuroscience* 1995; **67**: 177–188.
58. Mansour-Robaey S, Clarke DB, Wang YC, Bray GM, Aguayo AJ. Effects of ocular injury and administration of brain-derived neurotrophic factor on survival and regrowth of axotomized retinal ganglion cells. *Proc Natl Acad Sci USA* 1994; **91**: 1632–1636.
59. Clarke DB, Bray GM, Aguayo AJ. Prolonged administration of NT-4/5 fails to rescue most axotomized retinal ganglion cells in adult rats. *Vision Res* 1998; **38**: 1517–1524.
60. Mey J, Thanos S. Intravitreal injections of neurotrophic factors support the survival of axotomized retinal ganglion-cells in adult-rats *in vivo*. *Brain Res* 1993; **602**: 304–317.
61. Di Polo A, Aigner LJ, Dunn RJ, Bray GM, Aguayo AJ. Prolonged delivery of brain-derived neurotrophic factor by adenovirus-infected Muller cells temporarily rescues injured retinal ganglion cells. *Proc Natl Acad Sci USA* 1998; **95**: 3978–3983.
62. Cheng P, Sapieha P, Kitterlova WW, Hauswirth P, Di Polo A. TrkB gene transfer protects retinal ganglion cells from axotomy-induced death *in vivo*. *J Neurosci* 2002; **22**: 3977–3986.
63. McFarland TJ, Zhang Y, Appukuttan B, Stout JT. Gene therapy for proliferative ocular diseases. *Expert Opin Biol Ther* 2004; **4**: 1053–1058.
64. Kurokawa T, Katai N, Shibuki H, Kuroiwa S, Kurimoto Y, Nakayama C *et al*. BDNF diminishes caspase-2 but not c-Jun immunoreactivity of neurons in retinal ganglion cell layer after transient ischemia. *Invest Ophthalmol Vis Sci* 1999; **40**: 3006–3011.

65. Check E. A crucial test. *Nat Med* 2005; **11**: 243–244.
66. Kleinman ME, Yamada K, Takeda A, Chandrasekaran V, Nozaki M, Baffi JZ *et al*. Sequence- and target-independent angiogenesis suppression by siRNA via TLR3. *Nature* 2008; **452**: 591–597.
67. Sledz CA, Holko M, de Veer MJ, Silverman RH, Williams BR. Activation of the interferon system by short-interfering RNAs. *Nat Cell Biol* 2003; **5**: 834–839.
68. Bridge AJ, Pebernard S, Ducraux A, Nicolaz AL, Iggo R. Induction of an interferon response by RNAi vectors in mammalian cells. *Nat Genet* 2003; **34**: 263–264.
69. Reynolds A, Anderson EM, Vermeulen A, Fedorov Y, Robinson K, Leake D *et al*. Induction of the interferon response by siRNA is cell type- and duplex length-dependent. *RNA* 2006; **12**: 988–993.
70. Robbins M, Judge A, MacLachlan I. siRNA and innate immunity. *Oligonucleotides* 2009; **19**: 89–102.
71. Judge AD, Bola G, Lee AC, MacLachlan I. Design of noninflammatory synthetic siRNA mediating potent gene silencing *in vivo*. *Mol Ther* 2006; **13**: 494–505.
72. Lingor P, Koeberle P, Kugler S, Bahr M. Down-regulation of apoptosis mediators by RNAi inhibits axotomy-induced retinal ganglion cell death *in vivo*. *Brain* 2005; **128**: 550–558.
73. Lowenstein PR. Virology and immunology of gene therapy, or virology and immunology of high MOI infection with defective viruses. *Gene Ther* 2003; **10**: 933–934.
74. Hamar P, Song E, Kokeny G, Chen A, Ouyang N, Lieberman J. Small interfering RNA targeting Fas protects mice against renal ischemia-reperfusion injury. *Proc Natl Acad Sci USA* 2004; **101**: 14883–14888.
75. Cheng L, Sapieha P, Kittlerova P, Hauswirth WW, Di Polo A. TrkB gene transfer protects retinal ganglion cells from axotomy-induced death *in vivo*. *J Neurosci* 2002; **22**: 3977–3986.
76. Zhou HS, Liu DP, Liang CC. Challenges and strategies: the immune responses in gene therapy. *Med Res Rev* 2004; **24**: 748–761.
77. Gomes dos Santos AL, Bochet A, Fattal E. Intraocular delivery of oligonucleotides. *Curr Pharm Biotechnol* 2005; **6**: 7–15.
78. Nelson PT, Baldwin DA, Kloosterman WP, Kauppinen S, Plasterk RH, Mourelatos Z. RAKE and LNA-ISH reveal microRNA expression and localization in archival human brain. *RNA* 2006; **12**: 187–191.
79. Chen C, Ridzon DA, Broomer AJ, Zhou Z, Lee DH, Nguyen JT *et al*. Real-time quantification of microRNAs by stem-loop RT-PCR. *Nucleic Acids Res* 2005; **33**: e179.



Cell Death and Disease is an open-access journal published by Nature Publishing Group. This work is licensed under the Creative Commons Attribution-NonCommercial-No Derivative Works 3.0 Unported License. To view a copy of this license, visit <http://creativecommons.org/licenses/by-nc-nd/3.0/>

Supplementary Information accompanies the paper on Cell Death and Disease website (<http://www.nature.com/cddis>)